J|A|C|S ARTICLES

Published on Web 08/12/2009

Lateral Diffusion of Membrane Proteins

Sivaramakrishnan Ramadurai,[†] Andrea Holt,[‡] Victor Krasnikov,[†] Geert van den Bogaart,[†] J. Antoinette Killian,[‡] and Bert Poolman*[,†]

Department of Biochemistry, Groningen Biomolecular science and Biotechnology Institute & Zernike Institute of Advanced Materials, University of Groningen, Nijenborgh 4, 9747 AG Groningen, The Netherlands, and Chemical Biology and Organic Chemistry, Bijvoet Center for Biomolecular Research, Utrecht University, The Netherlands

Received April 9, 2009; E-mail: b.poolman@rug.nl

Abstract: We measured the lateral mobility of integral membrane proteins reconstituted in giant unilamellar vesicles (GUVs), using fluorescence correlation spectroscopy. Receptor, channel, and transporter proteins with 1−36 transmembrane segments (lateral radii ranging from 0.5 to 4 nm) and a α-helical peptide (radius of 0.5 nm) were fluorescently labeled and incorporated into GUVs. At low protein-to-lipid ratios (i.e., 10−100 proteins per μm^2 of membrane surface), the diffusion coefficient D displayed a weak dependence on the hydrodynamic radius (R) of the proteins [D scaled with $\ln(1/R)$], consistent with the Saffman-Delbrück model. At higher protein-to lipid ratios (up to 3000 μm^{-2}), the lateral diffusion coefficient of the molecules decreased linearly with increasing the protein concentration in the membrane. The implications of our findings for protein mobility in biological membranes (protein crowding of ∼25,000 μm^{-2}) and use of diffusion measurements for protein geometry (size, oligomerization) determinations are discussed.

Introduction

Biological membranes play a crucial role in many cellular processes, ranging from membrane transport and energy transduction to sensing and signal transduction to catalysis at the cell surface. According to the fluid mosaic model of Singer and Nicolson,[1] the biological membrane can be considered as a two-dimensional liquid in which lipid and protein molecules diffuse freely. We now know that not all membrane proteins diffuse freely as many are incorporated into large oligomeric or supramolecular complexes and/or they are anchored to the cellular skeleton.[2] Moreover, the distribution of the lipids in the bilayer is not homogeneous and discrete domains can be formed, such as liquid ordered domains that are enriched in cholesterol and saturated lipids versus liquid disordered domains that are enriched in unsaturated lipids.[3,4] These membrane microdomains may favor specific protein−lipid and protein−protein interactions by concentrating certain proteins, while excluding others.[5] Also, biological membranes are highly crowded and lipid-to-protein ratios on weight basis range from ∼0.35 (inner mitochondrial membrane) to ∼1 (plasma membrane) to >1 (secretory vesicles).[6] The membrane area fraction occupied by these proteins ranges from 15−35%.[7] This implies that a typical membrane protein with a perimeter of 15 nm is surrounded on average by a shell of lipids of only a few layers thick. Consequently, diffusing objects will be hindered in their mobility, but the magnitude of the effect is poorly studied.[8]

Lateral diffusion of integral and peripheral membrane proteins is an important factor in controlling the dynamics and functioning of the cell membrane.[9,10] In the 1970s, Saffman and Delbrück developed a continuum hydrodynamic model of lateral and rotational Brownian diffusion of proteins in lipid membranes.[11−13] The model treats the biological membrane as an infinite plane sheet of viscous fluid (lipid) separating infinite regions of less viscous liquid (water), and the embedded protein molecules are regarded as cylinders. In the model the lateral mobility of these cylinders along the membrane is described by their diffusion coefficient D and is only weakly (logarithmically) dependent on their lateral radius. The Saffman-Delbrück (SD) theoretical framework has in subsequent years been used to derive the radii of membrane proteins from diffusion measurements, for example, bacteriorhodopsin,[14] bovine rhodopsin, Ca^{2+}-activated adenosine triphosphatase, and acetylcholine receptor.[15] More recently, Gambin et al.[16] observed that lateral

[†] University of Groningen, the Netherlands.
[‡] Utrecht University, the Netherlands.

(1) Singer, S. J.; Nicolson, G. L. *Science* **1972**, *75*, 720.
(2) Kahya, N.; Schwille, P. *Mol. Memb. Biol.* **2006**, *23*, 29.
(3) Kahya, N.; Scherfeld, D.; Bacia, K.; Poolman, B.; Schwille, P. *J. Biol. Chem.* **2003**, *278*, 28109.
(4) Risselada, H. J.; Marrink, S. J. *Proc. Natl. Acad. Sci. U.S.A.* **2008**, *105*, 17367.
(5) Simons, K.; Toomre, D. *Nat. Rev. Mol. Cell Biol.* **2000**, *1*, 31.
(6) Zinser, E.; Sperka-Gottlieb, C. D.; Fasch, E. V.; Kohlwein, S. D.; Paltauf, F.; Daum, G. *J. Bacteriol.* **1991**, *173*, 2026.
(7) Dupuy, A. D.; Engelman, D. M. *Proc. Natl. Acad. Sci. U.S.A.* **2008**, *105*, 2848.
(8) Frick, M.; Schmidt, K.; Nichols, B. J. *Curr. Biol.* **2007**, *17*, 462.
(9) Axelrod, D. *J. Membr. Biol.* **1983**, *75*, 1.
(10) Ronchi, P.; Colombo, S.; Francolini, M.; Borgese, N. *J. Cell Biol.* **2008**, *18*, 105.
(11) Saffman, P. G.; Delbrück, M. *Proc. Natl. Acad. Sci. U.S.A.* **1975**, *72*, 3111.
(12) Saffman, P. G. *J. Fluid Mech.* **1976**, *73*, 593.
(13) Hughes, B. D.; Pailthorpe, B. A.; White, L. R. *J. Fluid Mech.* **1981**, *110*, 349.
(14) Peters, R.; Cherry, R. J. *Proc. Natl. Acad. Sci. U.S.A.* **1982**, *79*, 4317.
(15) Vaz, W. L. C.; Criado, M.; Madeira, V. M. C.; Schoellmann, G.; Jovin, T. M. *Biochemistry* **1982**, *21*, 5608.
(16) Gambin, Y.; Lopez-Esparza, R.; Reffay, M.; Sierecki, E.; Gov, N. S.; Genest, M.; Hodges, R. S.; Urbach, W. *Proc. Natl. Acad. Sci. U.S.A.* **2006**, *103*, 2098.

10.1021/ja902853g CCC: $40.75

diffusion of transmembrane peptides and proteins is more strongly dependent on their radii than suggested by the SD model. They determined the diffusion of transmembrane peptides, bacteriorhopdosin (BR) and lipids in a membrane-solvent system composed of penta-monododecylether (nonionic surfactant), of which the hydrophobic thickness was varied by inclusion of dodecane, and in 1-stearoyl-2-oleoyl-*sn*-glycero-3-phosphocholine (SOPC) vesicles, using a surface-supported bilayer configuration. The experimental diffusion coefficients differed several fold from the predictions of the SD model.[16] In an attempt to rationalize the apparent discrepancies, Naji et al.[17] pointed out that protein-induced membrane deformations can shift the mobility from an $\ln(1/R)$ (SD model) to a $1/R$ scaling. Recent coarse-grained simulations by Guigas and Weiss[18] suggested that the SD model holds for diffusion of membrane proteins with radii smaller than 7 nm, but fails for objects with larger dimensions. However, the experimental data of Gambin et al.[16] were obtained for molecules with radii in the range 0.5 to 3 nm. Hydrophobic mismatches between the transmembrane proteins and surrounding lipid chains may account for some deviations, but recent course-grained simulations suggest that these are only minor.[19] Despite a large number of theoretical papers on the diffusivity of transmembrane proteins and membrane inclusions (e.g., lipid rafts),[17−22] there is clear lack of experimental data on the mobility of membrane proteins (peptides and complex assemblies), analyzed systematically and under functionally active conditions.

Here, we report on the concentration- and size-dependence of diffusion of transmembrane peptides and integral membrane proteins reconstituted into the physiologically relevant lipid bilayers. We used DOPC/DOPG mixtures in which the proteins are functional. The lipid vesicles were converted into free-standing membranes (GUVs), avoiding possible limitations in diffusion due to interactions of the proteins with surface supports. Fluorescence Correlation Spectroscopy (FCS) has proven to be a powerful technique to study the diffusion of transmembrane proteins and lipids with single-molecule sensitivity.[23,24] FCS allows measurements of lateral diffusion at very low protein to lipid ratios, avoiding possible artifacts due to membrane crowding (e.g., aggregation). Using FCS, we determined the lateral mobility of a series membrane proteins with known dimensions, that are, the trimeric glutamate transporter (GltT with radius ∼4.0 nm),[25] the dimeric lactose transporter (LacS, ∼3.2 nm),[26] the monomeric lactose permease (LacY, ∼2.0 nm),[27] the pentameric mechanosensitive channel of large conductance (MscL, ∼2.5 nm),[28] the heptameric mechanosensitive channel of small conductance (MscS, ∼4.0 nm)[29] and the single transmembrane helix receptor synaptobrevin 2 (∼0.5 nm).[30] High resolution crystal structures are available for GltT, LacY, MscL and MscS.[25,27−29] In addition, we used the well-characterized synthetic peptide WALP23[31,32] with radius ∼0.5 nm.

Materials and Methods

Protein Purification and Labeling. Single cysteine mutants of the glutamate transporter GltT (Q412C) from *Bacillus stearothermophilus*,[33] the lactose transporter LacS (A635C) from *Streptococcus thermophilus*,[34] the mechanosensitive channel protein of large conductance MscL (K55C) from *Escherichia coli*,[34] and the mechanosensitive channel protein of small conductance MscS (A285C) from *Escherichia coli* were prepared by standard molecular biology methods. The lactose permease LacY C154G/S401C mutant from *Escherichia coli* was a gift of Prof. H. R. Kaback.[35] The SNARE protein synaptobrevin 2 (117C) mutant from *Rattus norvegicus* was a gift from Prof. R. Jahn.[36]

For protein expression, *E. coli* strain MC1061 (GltT, MscS), HB101 (LacS), PB104 (MscL), XL1-blue line (LacY) was grown in Luria Broth (LB), and, in the midexponential growth phase ($OD_{600} \approx 0.8$), the cells were induced for 2 h with 100 μg/L L-arabinose (for GltT and MscS) or 1 mM isopropyl-β-D-thiogalactopyranoside (IPTG; for MscL and LacY) and LacS was expressed as described previously.[37] The cells were harvested by centrifugation, resuspended to a final $OD_{600} \approx 100$ and lysed by a single passage through a French press at 20 000 psi. The membranes were collected by centrifugation at 180 000× *g* for 1 h at 4 °C, resuspended to a protein concentration of 20 mg/mL and solubilized for 30 min at 4 °C by using either 1% (w/v) *n*-dodecyl β-D-maltoside (DDM) (GltT, LacS, MscS), 2% DDM (LacY) or 1% (w/v) Triton X100 (MscL). The solubilizate was cleared by centrifugation for 15 min at 280 000× *g*, after which the solubilized proteins were purified by nickel affinity chromatography, essentially as described previously.[34] Solubilization buffers were 50 mM potassium phosphate (KPi), pH 8.0, 300 mM NaCl, 10% (w/v) glycerol, 15 mM imidazole (GltT); 50 mM KPi, pH 8.0, 100 mM NaCl, 10% (w/v) glycerol, 15 mM imidazole (LacS); 50 mM KPi, pH 8.0, 200 mM NaCl, 5 mM imidazole (LacY); 50 mM KPi, pH 8.0, 300 mM NaCl, 25 mM imidazole (MscL, MscS).[34] The solubilized material was incubated with Ni^{2+}-Sepharose resin for 1 h at 4 °C while rotating (25 mg of resin per 1 mg of total membrane protein). Subsequently, the resin was drained and washed with 20 column volumes of solubilization buffer containing 0.05% (w/v) DDM (GltT, LacS, MscS), 0.1% (w/v) Triton × 100 (MscL), or 0.01% (w/v) DDM (LacY), supplemented with 60 mM imidazole (GltT, MscS, MscL), 40 mM imidazole (LacS), or 25 mM imidazole (LacY). The proteins were labeled with Alexa fluor 488 (AF488, Invitrogen), while bound to the Ni^{2+}-sepharose resin, at a 1:30 molar ratio of protein over AF488. After incubation for 2 h, the column was washed with 20 column volumes of solubilization buffer without imidazole supplemented with 0.05% (w/v) DDM (GltT, LacS, MscS), 0.1% (w/v) Triton × 100 (MscL), 0.01% DDM

(17) Naji, A.; Levine, A. J.; Pincus, P. A. *Biophys. J.* **2007**, L49.
(18) Guigas, G.; Weiss, M. *Biophys. J.* **2006**, *91*, 2393.
(19) Guigas, G.; Weiss, M. *Biophys. J.* **2008**, L25.
(20) Schmidt, U.; Guigas, G.; Weiss, M. *Phys. Rev. Lett.* **2008**, *101*, 128104.
(21) Petrov, P. E.; Schwille, P. *Biophys. J.* **2008**, L41.
(22) Falck, E.; Róg, T.; Karttunen, M.; Vattulainen, I. *J. Am. Chem. Soc.* **2008**, *130*, 44.
(23) Schwille, P.; Korlach, J.; Webb, W. W. *Cytometry* **1999**, *36*, 176.
(24) Haustein, E.; Schwille, P. *Curr. Opin. Struct. Biol.* **2004**, *14*, 531.
(25) Yernool, D.; Boudker, O.; Jin, Y.; Gouaux, E. *Nature* **2004**, *431*, 811.
(26) Spooner, P. J.; Friesen, R. H. E.; Knol, J.; Poolman, B.; Watts, A. *Biophys. J.* **2000**, *79*, 756.
(27) Abramson, J.; Smirnova, I.; Kasho, V.; Verner, G.; Kaback, H. R.; Iwata, S. *Science* **2003**, *301*, 610.
(28) Chang, G.; Spencer, R. H.; Lee, A. T.; Barclay, M. T.; Rees, D. C. *Science* **1998**, *282*, 2220.
(29) Bass, R. B.; Strop, P.; Barclay, M. T.; Rees, D. C. *Science* **2002**, *298*, 1582.
(30) Bowen, M.; Brunger, A. T. *Proc. Natl. Acad. Sci. U.S.A.* **2006**, *103*, 8378.
(31) Holt, A.; de Almeida, R. F. M.; Nyholm, T. K. M.; Loura, L. M. S.; Daily, A. E.; Staffhorst, R. W. H. M.; Rijkers, D. T. S.; Koeppe, R. E., II; Prieto, M.; Killian, J. A. *Biochemistry* **2008**, *47*, 2638.
(32) Sparr, E.; Ganchev, D. N.; Snel, M. M. E.; Ridder, A. N. J. A.; Kroon-Batenburg, L. M. J.; Chupin, V.; Rijkers, D. T. S.; Killian, J. A.; De Kruijff, B. *Biochemistry* **2005**, *44*, 2.
(33) Slotboom, D. J.; Sobczak, I.; Konings, W. N.; Lolkema, J. S. *Proc. Natl. Acad. Sci. U.S.A.* **1999**, *96*, 14282.
(34) Doeven, M. K.; Folgering, J. H. A.; Krasnikov, V.; Geertsma, E. R.; van den Bogaart, G.; Poolman, B. *Biophys. J.* **2005**, *88*, 1134.
(35) Majumdar, D. S.; Smirnova, I.; Kasho, V.; Nir, E.; Kong, X.; Weiss, S.; Kaback, H. R. *Proc. Natl. Acad. Sci. U.S.A.* **2007**, *104*, 12640.
(36) Pabst, S.; Margittai, M.; Vainius, D.; Langen, R.; Jahn, R.; Fasshauer, D. *J. Biol. Chem.* **2002**, *277*, 7838.
(37) Veenhoff, L. M.; Geertsma, E. R.; Knol, J.; Poolman, B. *J. Biol. Chem.* **2000**, *275*, 23834.

(LacY) to remove free AF488 dye. Subsequently, the proteins were eluted with solubilization buffer containing 200 mM (LacY) or 400 mM (GltT, LacS, MscL, MscS) of imidazole.[34,35] The concentration of purified proteins was determined by the Bradford assay,[38] using bovine serum albumin (BSA) as a protein standard, and by measuring the absorbance at 280 nm, using extinction coefficients 0.625, 0.926, 1.169, and 0.823 $(mg/mL)^{-1}cm^{-1}$ for GltT, LacS, LacY, and MscS, respectively. The SNARE protein synaptobrevin 2 was expressed, purified, and fluorescently labeled as described in ref 36 except that buffers containing 1% sodium cholate were used. The endogenous cysteine (C103) located in the transmembrane helix was inaccessible for maleimide labeling.

The single transmembrane peptide WALP23 was synthesized as described previously.[31] For fluorescent labeling ca. 0.5 mg of peptide was dissolved in 200 μL trifluoroethanol and 10 μL H_20 was added, followed by 2 μL of triethylamine and 1.25 (peptide) equivalents of Alexa fluor 488 label dissolved in methanol. All solvents were purged with N_2 and the samples were kept under an N_2 atmosphere. After stirring the reaction mixture in the dark during 3 days at 4 °C, the peptides were precipitated in 10 mL of cold methyl *tert*-butyl ether/*n*-hexane (1:1 by volume) to remove unbound Alexa fluor 488 label. The precipitate was collected by centrifugation, and the precipitate was washed once again with methyl *tert*-butyl ether/*n*-hexane (1:1). The WALP23 peptide concentration was determined using an extinction coefficient of 22 400 $M^{-1}cm^{-1}$ at 280 nm in trifluoroethanol.[32] Peptide-bound Alexa fluor 488 absorption at 280 nm was corrected for by subtraction of the 280 nm absorbance of free label, which was scaled to equal intensity at the main absorbance band around 488 nm. From the peptide absorption spectra a typical labeling efficiency was estimated of 80−90%. The Alexa fluor 488-labeling of peptides and proteins was verified by MALDI/TOF mass spectrometry, using α-cyano-4-hydroxycinnaminic acid as matrix.

Vesicle Formation and Membrane Reconstitution. Large unilamellar vesicles (LUVs) were formed from DOPC/DOPG (3:1, mol/mol) (Avanti polar lipids, USA) with 0.001% mol/mol of the lipid probe 1,1′-dioctadecyl-3,3,3′,3′-tetramethylindo-dicarbocyanine perchlorate (DiD) (Invitrogen; excitation maximum at 644 nm, emission at 665 nm). Forty milligrams of lipid mixture was dried in a rotary evaporator to remove the chloroform, as described previously.[34] The thin film of dried lipids was rehydrated to a total concentration of 10 mg of lipid/mL with 50 mM KPi, pH 7.0, and, subsequently, the lipids were flash frozen in liquid nitrogen and thawed at room temperature, three times. Prior to membrane reconstitution, the multilamellar vesicles, obtained after freezing-thawing, were extruded through 400 nm polycarbonate filters to obtain LUVs. Next, the LUVs were titrated stepwise with 10 μL aliquots of 10% Triton X-100;[39] typically 80 μL of 10% Triton X-100 was used per 1 mL of LUVs. The purified proteins or the WALP23 peptide were added to the detergent-destabilized LUVs at 1:150 protein:lipid ratio (w/w), unless indicated otherwise. The detergent−lipid−protein complex was incubated while gently shaking for 45 min at room temperature. The mixture was then incubated with 40 mg of polystyrene beads (Bio-Beads SM2 from Bio-Rad Inc.)/mg of detergent[40] to remove the detergent. Subsequently, the proteo-LUVs were dried under vacuum in the presence of 5% ethylene glycol (v/v) for at least 12 h, and giant unilamellar vesicles (GUVs) were formed as reported previously.[34] Briefly, the dried lipid film was rehydrated in 10 mM KPi, pH 7.0, and GUV formation was monitored on a confocal microscope.

Fluorescence Correlation Spectroscopy (FCS). Measurements were carried out on a dual-color laser scanning confocal microscope[34] based on an inverted microscope Axiovert S 100 TV (Zeiss) in combination with a galvanometer optical scanner (model 6860, Cambridge technology) and a microscope objective nanofocusing device (P-721, PI). The two laser beams, the 488 nm argon ion laser (Spectra Physics) and 633 nm He−Ne laser (JDS Uniphase), were focused by a Zeiss C-Apochromat infinity-corrected 1.2 NA 40× water immersion objective for excitation of the Alexa Fluor 488 and DiD fluorophores. The fluorescence was collected through the same objective, separated from the excitation beams by a beam-pick off plate (BSP20-A1, Thor-Laboratories), and finally directed through emission filters (HQ 550/100 and HQ675/50, Chroma technology) and pinholes (diameter 30 μm) onto two avalanche photodiodes (SPCM-AQR-14, EG&G). The fluorescence signals were digitized and auto- and cross-correlation curves were calculated using a multiple τ algorithm.

The autocorrelation function $G(\tau)$ was calculated from the intensity trace as follows:

$$G(\tau) = \frac{\langle \delta F(t) \cdot \delta F(t+\tau) \rangle}{\langle F(t) \rangle^2} \quad (1)$$

where F is the fluorescence intensity, t is the time, and τ is the lag time; the angular brackets refer to time averaging, so that $\delta F(t) = F(t) - \langle F(t) \rangle$. The diffusion of fluorescent particles within lipid membrane occurs in two dimensions. The autocorrelation curve was fitted using the following two-dimensional diffusion model:[41]

$$G_D(\tau) = \frac{1}{N}\left(1 + \frac{\tau}{\tau_D}\right)^{-1} \quad (2)$$

where N is the average number of fluorescent particles in the detection area. The diffusion time τ_D is related to the diffusion coefficient D through the expression:

$$\tau_D = \frac{\omega^2}{4D} \quad (3)$$

where ω is lateral radii, defined as the point were the fluorescence count rate dropped e^2 times.The setup was calibrated by measuring the known diffusion coefficients of Alexa fluor 488 and 633 in water (Invitrogen; $D = 380$ $\mu m^2 s^{-1}$[42]). The lateral radii, ω, were 200 nm for Alexa fluor 488 and 270 nm for Alexa fluor 633. The detailed fitting procedure (Figure S1−S3), incl. photophysical properties of the fluorophores, and the membrane fluctuations (Figure S4) are explained in the Supporting Information. Error bars in figures and text (±values) refer to standard deviations obtained from diffusion measurements of at least 3 independent data sets each consisting of 7−10 measurements.

Results and Discussion

Production, Purification and Fluorescent Labeling of Membrane Proteins. The six model membrane proteins used in this study are the glutamate transporter GltT from *Bacillus stearothermophilus*,[33] the lactose transporter LacS from *Streptococcus thermophilus*, the mechanosensitive channel protein of large conductance MscL from *Escherichia coli*,[34] the mechanosensitive channel protein of small conductance MscS from *Escherichia coli*, the lactose permease LacY from *Escherichia coli*,[35] and the SNARE protein synaptobrevin 2 from *Rattus norvegicus*.[36] In order to selectively label the proteins with fluorescent probes for detection by confocal imaging and FCS measurements, single-cysteine residues were engineered (except for LacY). The positions of the cysteine residues were located either near the C-terminus of the protein (LacS, GltT), the N-terminus (MscS, Synaptobrevin 2) or in an extracellular loop (MscL). In the case of the LacY mutant [LacY(C154G/S401C)],

(38) Bradford, M. M. *Anal. Biochem.* **1976**, *72*, 248.
(39) Knol, J.; Veenhoff, L. M.; Liang, W. J.; Henderson, P. J.; Leblanc, G.; Poolman, B. *J. Biol. Chem.* **1996**, *271*, 15358.
(40) Girard, P.; Pécréaux, J.; Lenoir, G.; Falson, P.; Rigaud, J.-L.; Bassereau, P. *Biophys. J.* **2004**, *87*, 419.
(41) Elson, E. L.; Magde, D. *Biopolymers* **1974**, *13*, 1.
(42) Petrášek, Z.; Schwille, P. *Biophys. J.* **2008**, *94*, 1437.

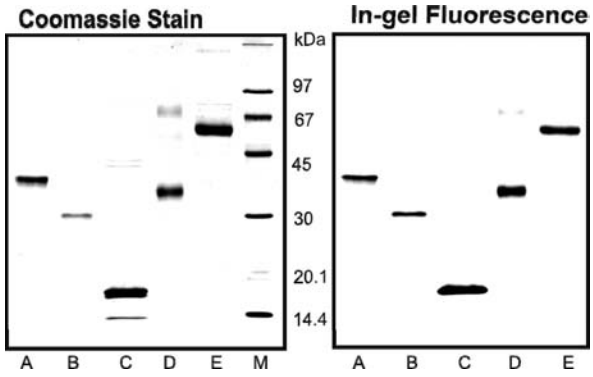

Figure 1. SDS-PAGE analysis of purified and AF 488-labeled cysteine mutants. Purified proteins labeled with Alexa Fluor 488 C5 maleimide (Invitrogen) were visualized by fluorescence emission (right-hand panel) and subsequently stained with Coomassie brillant blue (left-hand panel). Cysteine-substituted proteins used were GltT (Q412C) [A], MscS (A285C) [B], MscL (K55C) [C], LacY (C154G/S401C) [D], LacS (A635C) [E], molecular weight marker [M]. For LacY (lane D), some dimeric protein can be seen which is an artifact of the sample treatment and frequently observed with SDS-PAGE.[45]

the cysteine at position 401 is located at the cytoplasmic end of helix XII. The LacY(C154G/S401C) was labeled specifically at Cys-401 by adding 15 mM 4-nitrophenyl α-D-galactopyranoside (Sigma Aldrich) to protect the native Cys-148 from alkylation, as described previously.[34] The cysteine in each of the membrane proteins was labeled with Alexa fluor 488 C5 maleimide (AF488), and unbound labels were removed by extensive washing of the proteins while bound to the nickel affinity resin. After metal-affinity chromatography, LacS was further purified on a Sephadex 200 size-exclusion column. The degree of labeling with AF488 of the proteins was estimated by measuring the AF488 absorbance (extinction coefficient is 71 000 $M^{-1}cm^{-1}$ at 495 nm) and relating this to the protein concentration as determined by the Bradford assay. The labeling efficiency was found to be 60−75% for each protein. Figure 1 shows the in-gel fluorescence and Coomassie staining of an SDS-PAGE gel of purified and Alexa fluor 488-labeled proteins. The proteins were found >95% pure on the basis of Coomassie staining. Each of the membrane proteins was reconstituted into LUVs composed of a 3:1 molar ratio of DOPC and DOPG. For the channel and transport proteins, it has been shown that anionic lipids are required for activity or increase the fraction of functionally reconstituted protein (LacS,[34] GltT [data not shown], LacY,[43] MscL[34] [data not shown], MscS[44]). DOPG was not only required for activity of the transporter proteins but also promoted the GUV formation.[34]

Confocal Imaging of Membrane Proteins in GUVs. The AF488-labeled proteins were reconstituted into Triton X-100 destabilized LUVs composed of DOPC:DOPG in 3:1 ratio. For FCS measurements, the GUVs were prepared by drying the LUVs in the presence of stabilizing amounts of ethylene glycol (or sucrose; see ref 34 for details on the protein-stabilizing effects of the cosolvents) and rehydrated in aqueous buffer. GUV formation was monitored by means of confocal microscopy (Figure 2A), using the fluorescent labels of the protein and DiD.

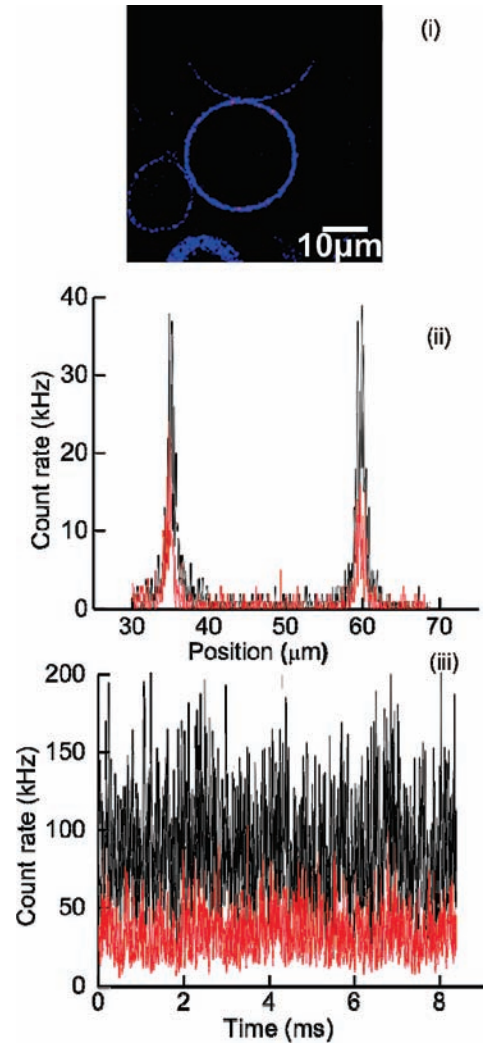

Figure 2. Liposomes prepared from DOPC/DOPG (3:1 molar ratio) and labeled with 1:153 000 (mol/mol) of the fluorescent lipid analog DiD and 1:20 000 mol/mol protein-to-lipid ratio of Alexa fluor 488 labeled GltT. (i) $x-y$ confocal microscopy image of a GUV; (ii) z-confocal scan, the laser beams were focused on the GUV pole (right-hand peak); (iii) typical fluctuations over time of the fluorescent signals. The black and red spikes in panels (ii) and (iii) correspond to fluorescence fluctuations of DiD and AF488-labeled protein, respectively.

These images confirm that the proteins were distributed homogeneously into the GUVs, at least at the optical resolution scale. To accurately position the focal volume on the pole of the GUV, a z-scan, that is parallel to the optical axis, was performed (Figure 2B). Next, the fluctuations of the fluorescence signals in both channels, $F_1(t)$ and $F_2(t)$ (Figure 2C) were recorded. The time-dependent fluctuations of $F_1(t)$ and $F_2(t)$ were evaluated by calculating the autocorrelation functions $G(\tau)$. A typical autocorrelation function is shown in Figure 3. The obtained autocorrelation functions $G(\tau)$ could be fitted reasonably well to a one-component two-dimensional diffusion model, yielding values of the protein and DiD diffusion coefficients. Only GUVs with diameters of 15−40 μm were used for the measurements, in order to avoid undulations in the case of larger GUVs and to avoid possible curvature effects in the case of smaller vesicles.

Concentration-Dependent Lateral Diffusion of Proteins. To evaluate the effect of protein crowding on lateral diffusion of proteins and lipids, we prepared GUVs with GltT, LacS and

(43) Picas, L.; Merino-Montero, S.; Morros, A.; Hernández-Borrell, J.; Teresa Montero, M. *J. Fluoresc.* **2007**, *17*, 649.
(44) Valeria, V.; Marien Cortes, D.; Furukawa, H.; Perozo, E. *Biochemistry* **2007**, *46*, 6766.
(45) Carrasco, N.; Tahara, S. M.; Patel, L.; Goldkorn, T.; Kaback, H. R. *Proc. Natl. Acad. Sci. U.S.A.* **1982**, *79*, 6894.

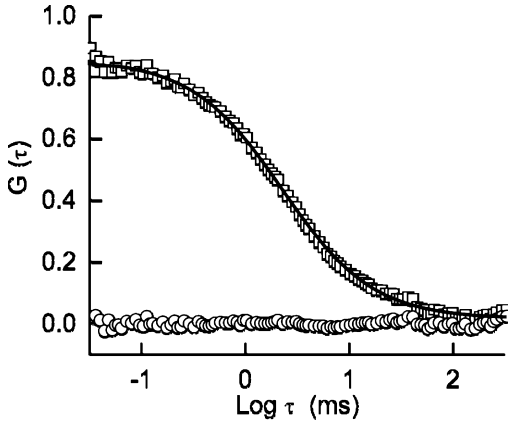

Figure 3. Typical autocorrelation function (□) for proteins/peptide in GUVs. The data correspond to AF488-labeled GltT (Q412C) reconstituted at 1:20 000 mol/mol protein-to-lipid ratio. The solid line is a fit to the one-component two-dimensional diffusion model (eq 2) with number of particles N of 1.2, diffusion time τ_D of 2.255 ms, and corresponding diffusion coefficient D of 3.6 $\mu m^2 s^{-1}$; the residuals of the fit are shown.

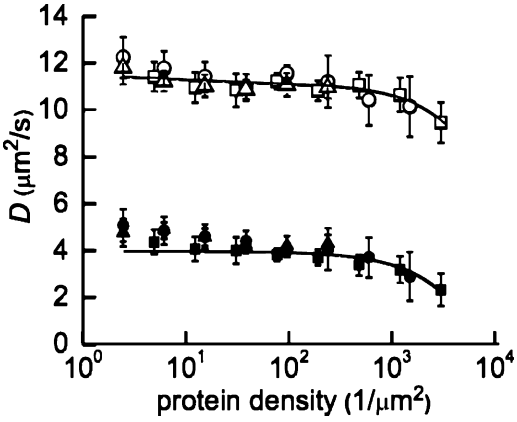

Figure 4. Lateral diffusion of protein and lipids as a function of protein density in the membrane. The labeled proteins were reconstituted in liposomes composed of DOPC/DOPG (3:1) at various protein-to-lipid ratios. The data were grouped in 9 bins logarithmically spread over the measured protein-to-lipid range. Each bin consists of at least 10 liposomes. The diffusion coefficients are shown for GltT (■) and lipids (□); LacS (●) and lipids (○); LacY (▲) and lipids (Δ). The solid lines are linear fits for GltT (■,□).

LacY at different protein-to-lipid ratios, that is, from 1:15 000 to 1:20 on weight basis and corresponding to approximate molar ratios of $1:3 \cdot 10^6$ to 1:4000 for trimeric GltT and dimeric LacS and $1:10^6$ to 1:1,500 for monomeric LacY. To avoid too many fluorescent particles in the confocal volume, only a fraction of the proteins was labeled with AF488; labeled and unlabeled proteins were mixed at the appropriate ratios. Figure 4 presents the protein and lipid diffusion coefficients D as a function of protein density in the membrane. The protein densities were calculated from FCS autocorrelation functions and did not completely follow the initial protein-to-lipid ratios, which could be due to variations in the reconstitution efficiency and inhomogeneous formation of GUVs during the rehydration. The data were pooled into 9 bins with at least 10 liposomes per bin. Similar to previous reports,[46−50] the diffusion coefficients of the proteins and the lipids decreased linearly with increasing protein-to-lipid ratio. As an example, the solid lines in Figure 4 correspond to fits of a linear dependency of the GltT protein concentration. At very low protein-to-lipid ratios (<10 μm^{-2}), the data for LacS deviated from the linear dependence, possibly due to dissociation of the dimeric complex into monomers.[51] The data summarized in figure 4 show that protein crowding does influence the diffusion coefficient of proteins. However, at a protein density below 100 μm^{-2}, the effect of protein crowding is small and was ignored in the measurements aimed at probing the size-dependence of the protein mobilities. Because the protein mobility was affected by the crowding of the membrane, the data were analyzed for anomalous diffusion (Supporting Information Figures S5−S7). The anomality parameter α decreased from 0.95 ± 0.05 to 0.88 ± 0.03 when the protein-to-lipid ratio increased from 5 to 3000 proteins/μm^2. Thus, even at the highest protein crowding conditions, the degree of anomality of protein diffusion was small.

Size-Dependent Lateral Diffusion of Proteins. The lateral diffusion was measured using FCS of the trimeric glutamate transporter (GltT; lateral radius ∼ 4 nm), the dimeric lactose transporter (LacS; ∼3.2 nm), the monomeric lactose permease (LacY; ∼2 nm), the heptameric mechanosensitive channel of small conductance (MscS; ∼4 nm), the pentameric mechanosensitive channel of large conductance (MscL; ∼2.5 nm), synaptobrevin 2 (radius > 0.5 nm), and the synthetic peptide WALP23 with a single transmembrane helix of radius 0.5 nm. The radii of the proteins were obtained from their crystal structures, except for LacS, whose radius was taken from measurements and models described in Spooner et al.,[26] and for WALP23, which was based on the interhelical peptide−peptide distance as determined by X-ray diffraction on linear peptide aggregates in lipid bilayers.[32] For synaptobrevin 2, the hydrodynamic radius was inferred from infrared dichroism data.[30] Figure 5 presents the measured diffusion coefficient of the proteins as a function of their radius. Each measurement was carried out at least 3 times (independent protein isolations and reconstitutions) with at least 10 liposomes each.

The fluorescent lipid probe DiD was incorporated with the proteins during the preparation of LUVs. The lateral diffusion coefficient of lipids D in GUVs and proteo-GUVs (for all measured proteins in the concentration range from 1 up to 10 μm^{-2}) were determined to be 11.3 ± 0.6 $\mu m^2 s^{-1}$ and 11.4 ± 0.7 $\mu m^2 s^{-1}$, respectively. This indicates that at the protein to lipid ratios used, the membrane proteins did not significantly affect the mobility of the lipids.

The lateral diffusion of the proteins only weakly depended on the radius (open circles in Figure 5), as postulated by Saffman and Delbrück in their continuum hydrodynamic model.[11] The SD model predicts that the lateral diffusion coefficient D of membrane protein is relatively insensitive to the radius R of the diffusing object:

$$D = \frac{k_B T}{4\pi\mu h}\left(\ln\left(\frac{\mu h}{\mu' R}\right) - \gamma\right) \quad (4)$$

where k_B is the Boltzmann constant, T is absolute temperature, h is the thickness of the bilayer, μ is viscosity of the membrane,

(46) Scalettar, B. A.; Abney, J. R.; Owicki, J. C. *Proc. Natl. Acad. Sci. U.S.A.* **1988**, *85*, 6726.
(47) Abney, J. R.; Scalettar, B. A.; Owicki, J. C. *Biophys. J.* **1989**, *55*, 817.
(48) Pink, D. A.; Laidlaw, D. J.; Chisholm, D. M. *Biochim. Biophys. Acta* **1986**, *863*, 9.
(49) Pink, D. A. *Biochim. Biophys. Acta* **1985**, *818*, 200.
(50) O'Leary, T. J. *Proc. Natl. Acad. Sci. U.S.A.* **1987**, *84*, 429.
(51) Friesen, R. H. E.; Knol, J.; Poolman, B. *J. Biol. Chem.* **2000**, *275*, 33527.

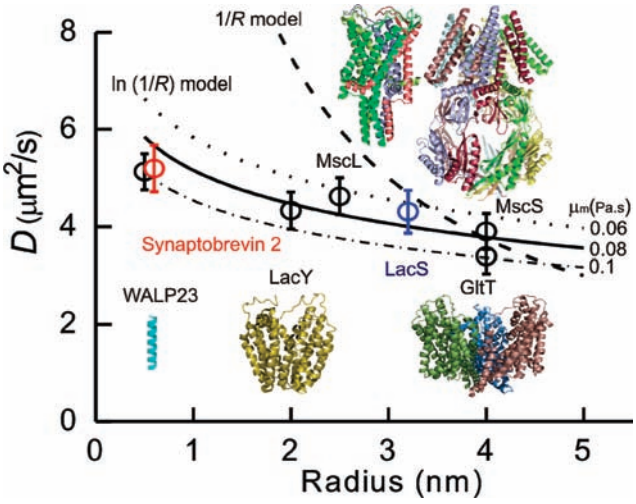

Figure 5. Size-dependent lateral diffusion of integral membrane proteins and peptides. The diffusion coefficient of proteins and peptide is plotted versus their lateral radius; the crystal structures of the membrane proteins are depicted in the figure, except for synaptobrevin 2 (red symbol) and LacS (blue symbol). The solid line presents the fit of the data to the Saffman-Delbrück [ln(1/*R*)] model, resulting in a value for $\mu h/\mu'$ of 325 nm (membrane viscosity, μ, of 0.08 Pa.s; μ' of 1.003 Pa.s; and h of 3.8 nm). The dotted and dot-dash lines represent the curves for values of μ of 0.06 and 0.1 Pa.s, yielding $\mu h/\mu'$ of 250 and 375 nm, respectively. For comparison, the curve for the 1/*R* model is also shown.

μ' is viscosity of the outer liquid, and γ is Euler's constant. According to the SD model, D of a membrane protein of radius R is determined by a single parameter ($\mu h/\mu'$). The solid line in Figure 5 presents the SD fit for the measured D values, resulting in a value for the parameter ($\mu h/\mu'$) of 325 nm. To estimate the sensitivity of the SD model to this parameter, two additional curves representing approximately ±20% deviation of the parameter and corresponding to ($\mu h/\mu'$) of 250 and 375 nm are shown in Figure 5. All data points are between these two lines suggesting that the SD model is able to predict the diffusion coefficient with better than 20% accuracy, providing known R, μ and h. As the thickness of the model membrane is around 4 nm,[52] the parameter ($\mu h/\mu'$) of 325 nm yields the membrane viscosity of 0.08 Pa·s. This value falls in a broad range of the reported membrane viscosities, and is close to a membrane viscosity estimate of 0.1 Pa·s often used in the literature.[53]

The continuum hydrodynamic SD model approximates the membrane as an infinite plane sheet of viscous fluid (lipids) separating infinite regions of less viscous liquid (water). The protein molecules are considered as incompressible, cylindrical inclusions in a membrane. Obviously, membrane proteins are not perfect cylindrical entities and the membrane structure is far more complex than an ideal plane sheet. Moreover, the bilayer thickness can be perturbed on protein insertion, which depends on hydrophobic match/mismatch between proteins and lipids. To compensate the mismatch, the lipid molecules closest to the protein will stretch out or compress in order to cover the hydrophobic core of the protein.[54,17] In the case of gramicidin A, used at very high peptide-to-lipid ratios of 1:10 on mole basis, the hydrophobic bilayer thickness of DPPC increased from 25.4 to 25.9 Å, which shows that lipids near the proteins tend to deform, compensating the hydrophobic mismatch.[55] Although such deformations of the membrane may occur in the layers of lipids surrounding the membrane proteins, the protein-to-lipid ratios used in our study were much lower than that in,[55] preventing the overall membrane thickening. As far as local deformations are concerned, recent coarse-grained simulations on the effect of hydrophobic mismatch between transmembrane proteins and the surrounding lipids showed that the mobility can be slowed, but the size-dependence of the diffusion coefficient is still consistent with the hydrodynamic model of Saffman and Delbrück.[19] Importantly, the dioleoyl [*cis*-18:1(9)] lipids used in our study support high activity of the proteins (investigated for LacY[56] and LacS, unpublished) or stabilize the closed conformation of the channels (MscS and MscL[42]), making it unlikely that hydrophobic mismatch will have contributed significantly. Considering all simplifications, the agreement between the SD model and the measured diffusion coefficients (Figure 5) is excellent.

Gambin and co-worker[16] determined the lateral mobility of synthetic model peptides reconstituted into bilayers made of nonionic surfactants. They observed that the lateral mobility was strongly radius-dependent. Generalizing their results, they proposed that the lateral mobility of membrane proteins is inversely proportional to their radius R (1/R model):

$$D = \frac{k_B T \lambda}{4\pi\mu h R} \tag{5}$$

where the symbols are the same as those in eq 4, except for λ which refers to a characteristic length to satisfy dimensionality. As shown in Figure 5, the measured radius dependence of D significantly deviates from the 1/R model. Attempts to determine the radius of the diffusing protein on the basis of the 1/R model would result in unacceptable errors.

The exact cause of the strong discrepancy with the SD model reported in[16] is not clear. The hydrophobic mismatch between BR and the SOPC membrane will have been negligible and cannot explain the discrepancy. We feel that the differences are related to the sample preparation technique, namely the formation of a surface-supported bilayer. The diffusion studies on cytochrome b5,[57] annexin V,[57] integrin receptors $\alpha_{IIb}\beta_3$[58] in supported bilayer systems show that 25% of the molecules were mobile. In other words, three-quarter of protein molecules are immobilized by the underlying support.[59] It is known that undesirable interactions between protein parts, protruding the membrane, and surfaces or interactions between lipids and supports slow down the diffusion,[57,58] which will give rise to anomalous diffusional behavior. In fact, the diffusion coefficients reported by Gambin and colleagues[16] for peptides and protein (bacteriorhodoposin) in SOPC lipids are at least an order of magnitude lower than generally observed.[60] Usually, the diffusion coefficient of BR and transmembrane proteins of

(52) Gallová, J.; Uhríková, D.; Kučerka, N.; Teixeira, J.; Balgavý, P. *Biochim. Biophys. Acta* **2008**, *1778*, 2627.
(53) Vaz, W. L. C.; Goodsaid-Zalduondo, F.; Jacobson, K. *FEBS Lett.* **1984**, *174*, 199.
(54) Jensen, M. Ø.; Mouritsen, O. G. *Biochim. Biophys. Acta* **2004**, *1666*, 205.
(55) de Planque, M. R. R.; Greathouse, D. V.; Koeppe, R. E.; Schfer, H.; Marsh, D.; Killian, J. A. *Biochemistry* **1998**, *37*, 9333.
(56) Le Coutre, J.; Narasimhan, L. R.; Patel, C. K. N.; Kaback, H. R. *Proc. Natl. Acad. Sci. U.S.A* **1997**, *94*, 10167.
(57) Tamm, L. K.; Wagner, M. L. *Biophys. J.* **2000**, *79*, 1400.
(58) Goennenwein, S.; Tanaka, M.; Hu, B.; Moroder, L.; Sackmann, E. *Biophys. J.* **2003**, *85*, 646.
(59) Diaz, A. J.; Albertorio, F.; Daniel, S.; Cremer, P. S. *Langmuir* **2008**, *24*, 6820.
(60) Deverall, M. A.; Gindl, E.; Sinner, E.-K.; Besir, H.; Ruehe, J.; Saxton, M. J.; Naumann, C. A. *Biophys. J.* **2005**, *88*, 1875.

comparable radii is approximately twice smaller than that of the lipids.[14,60] Our results corroborate this rule. Indeed, at the concentration of 10 μm^{-2} the measured diffusion coefficient ($D = 4.3 \pm 0.4\ \mu m^2 s^{-1}$) of LacY (radius of 2 nm) is approximately twice smaller than that ($D = 11.0 \pm 0.6\ \mu m^2 s^{-1}$) of the lipids. In the case of the penta-monododecylether ($C_{12}E_5$)-dodecane bilayer mimic, in addition to probable membrane-support interactions, several other factors may have enhanced and modified the diffusional anomalies, such as the inclusion of organic solvent, possible complications arising from the use of a sponge phase, and the local membrane deformations caused by the hydrophobic mismatch.

In conclusion, we show that integral membrane proteins, reconstituted into physiologically relevant phospholipids bilayers, diffuse with speeds that are only weakly dependent on their lateral radii, in agreement with the Saffman-Delbrück model. On the contrary, the recently proposed $1/R$ model failed even qualitatively to describe the size-dependent diffusion. The $\ln(1/R)$ dependence of D implies that diffusion measurements do not resolve changes in geometry (helix tilting) or size (monomer−dimer, protein−protein interactions) of membrane proteins, unless the changes (multimerization of protein) are very large. The effect of membrane crowding resulted in a linear decrease of the protein and lipid lateral diffusion coefficient with increasing protein concentration in the membrane. Extrapolating the data to protein densities of ~25 000 proteins per μm^2 (i.e., an area occupancy of 30% and typical for many biological membranes) would yield diffusion coefficients that are at least an order of magnitude lower than measured at 3000 μm^{-2} in the GUVs, consistent with FRAP measurements in plasma membranes in mammalian cells.[8] For objects that need to traverse large distances in cell (or organellar) membranes or when dynamic processes like protein association−dissociation are required for activity, such a slow diffusion could be a rate-determining factor.

Abbreviations: AF488, Alexa Fluor 488 C5 maleimide; DOPC, 1,2-dioleoyl l-*sn*-glycero-3-phosphocholine; DOPG, 1,2-dioleoyl-*sn*-glycero-3-[phospho-*rac*-(1-glycerol)]; DMPC, 1,2-dimyristoyl-*sn*-glycero-3-phosphocholine; DPPC, 1,2-dipalmitoleoyl-*sn*-glycero-3-phosphocholine; DiD, 1,1′-dioctadecyl-3,3,3′,3′-tetramethylindodicarbocyanine perchlorate; FCS, fluorescence correlation spectroscopy; GUVs, giant unilamellar vesicles; LUVs, large unilamellar vesicles; SD, Saffman-Delbrück; SOPC, 1-stearoyl-2-oleoyl-*sn*-glycero-3-phosphocholine.

Acknowledgment. We acknowledge financial support from NWO (Top-subsidy grant 700.56.302), SysMo via the BBSRC-funded KosmoBac programme coordinated by Ian R Booth (Aberdeen), a Marie Curie Early Stage Research Training Fellowship (Biomem-MEST-CT 2004-007931) for A.H. within the European Community's Sixth Framework Program, and the Zernike Institute for Advanced Materials for the financial support. We thank Prof. H.R. Kaback for a gift of LacY (plasmid pT7-5) and Prof. R. Jahn for a gift of synaptobrevin 2 (plasmid pET28a).

Supporting Information Available: The detailed fitting procedure including photophysical properties of the fluorophores, the membrane fluctuations, and the analysis of anomalous diffusion for protein mobility in crowded membrane are provided. This material is available free of charge via the Internet at http://pubs.acs.org.

JA902853G